Pergamon

Int. Comm. Heat Mass Transfer, Vol. 24, No. 7, pp. 965–976, 1997

0735-1933/97 $17.00 + .00

PII S0735-1933(97)00082-1

THREE DIMENSIONAL LAMINAR NON-NEWTONIAN FLUID FLOW AND HEAT TRANSFER IN THE ENTRANCE REGION OF A CROSS-SHAPED DUCT

S.Gh. Etemad
Dept. of Chemical Engineering, Isfahan University of Technology, Isfahan, Iran

(Communicated by J.P. Hartnett and W.J. Minkowycz)

ABSTRACT

The Galerkin finite element is used to solve the three dimensional momentum and energy equations for laminar non-Newtonian flow in cross-shaped straight duct. Both flow and heat transfer develop simultaneously from the entrance of the channel. Uniform wall temperature (T) and also constant wall heat flux both axially and peripherally (H2) are used as thermal boundary conditions. The power-law model is chosen to characterize the non-Newtonian behaviour of the fluid. The effect of power-law index and geometric parameter on the apparent friction factor as well as Nusselt number are presented and discussed.

Introduction

Many important industrial fluids are non-Newtonian in their flow characteristics. These include food materials, soap and detergent slurries, polymer solutions and many others. In the most of the industries such as polymer, foods, petrochemical the heat exchanger is an especially important component of the processing equipment. In the design of heat exchanger, the prediction of the heat transfer coefficient plays a key role as a design factor. At the inlet of tubes of heat exchangers, both hydrodynamic and thermal boundary layers develop simultaneously and most of the pressure drop and heat transfer occur in the entrance region of the channel. Therefore, simultaneously developing flow and heat transfer is important for many engineering applications.

Compact heat exchangers are preferred over shell and tube types because of substantial volume, weight and cost saving. A large number of heat transfer surfaces are available for choice and hence a proper selection of a surface is one of the most important factor in compact heat exchanger design. A summary of the Newtonian flow and heat transfer through arbitrary ducts has been presented by Shah and London [1] and Shah and Bhatti [2]. For non-Newtonian fluids extensive and comprehensive reports are provided by Cho and Hartnett [3], Hartnett and Kostic [4], Lawal and Mujumdar [5], and Etemad [6].

This numerical study in concerned with the simultaneously developing flow and heat transfer of Newtonian and power-law model non-Newtonian fluid flowing through cross-shaped channel. This duct can be as a possible candidate for compact heat exchangers.

Problem Statement

Fig. 1 presents the cross section of the cross-shaped duct. The origin of the coordinate systems is at the middle of bottom plate of the channel. Using the appropriate symmetry condition, the solution obtained for only half of the duct. A geometric parameter, λ, is defined (Fig. 1) which $\lambda = 0$ corresponds to square duct. The mesh generated for the finite element simulation of cross-shape duct with different λ are presented in Fig. 2(a-b). For channel with $\lambda = 0.25$, $61 \times 11 \times 21$ and for $\lambda = 0.50$, $61 \times 13 \times 25$ grids of 27 node quadratic elements were used to discretize the flow domain. The number of meshes was based on the requirement of mesh independence of the numerical solution. Due to the higher velocity and temperature gradients in the entrance region and in the vicinity of the walls, finer mesh distribution was used in these regions.

The flow and heat transfer is governed by the conservation equations of continuity, momentum, and energy. The flow and heat transfer are studied under the following assumptions: laminar, steady state, constant physical properties, and negligible viscous dissipation. The governing equations are nondimensionalized using the following dimensionless variables :

$$U = \frac{u}{u_e}, \quad V = \frac{v}{u_e}, \quad W = \frac{w}{u_e}$$
$$X = \frac{x}{D_h}, \quad Y = \frac{y}{D_h}, \quad Z = \frac{z}{D_h}, \quad P = \frac{p - \rho g z}{\rho u_e^2} \qquad (1)$$

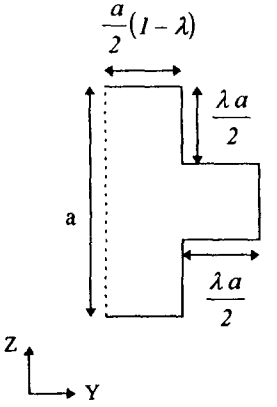

FIG. 1
Configuration of the cross-shaped channel

where the subscript e indicates entrance conditions.

For the constant wall temperature (T) : $\theta = \dfrac{T - T_w}{T_e - T_w}$

For the constant wall heat flux both axially and peripherally (H2): $\theta = \dfrac{T - T_e}{\dfrac{qD_h}{K}}$

The fluid enters the duct at uniform temperature and velocity. The no-slip condition is applied at the channel walls. In this numerical study attention is given to uniform wall temperature everywhere (T) and uniform heat flux axially as well as peripherally (H2) as thermal boundary conditions. For T boundary condition the dimensionless temperature at walls is zero while for H2 boundary condition the dimensionless heat flux at the heated walls is unity. The gradient of all dependent variables across the symmetry plane are zero except for the velocity perpendicular to the symmetry plane while the velocity itself at the symmetry plane is zero. A fully developed condition could be prescribed at the outlet boundary due to the long axial length of the plane.

The dimensionless governing equations which is a systems of highly nonlinear partial differential equations with associated boundary conditions were solved using FIDAP (a fluid dynamics and heat transfer analysis package based on Galerkin finite element method). The penalty approach was chosen for pressure with penalty parameter set at 10^{-8} to satisfy continuity without solving an additional partial differential equation. The streamline upwinding formulation was used to improve the probable numerical oscillation. Due to the high radius of convergence of the fixed iteration method and also the high rate of convergence of the quasi-Newton Raphson method, a combination strategy used to solve the algebraic equations, which starts with the fixed iteration method and then switches to the quasi-Newton Raphson approach. The combination strategy results in a significant saving in computational time. The solution and residual vectors were used as the criteria for convergence. In this study the tolerance level 10^{-4} was chosen for convergence criteria.

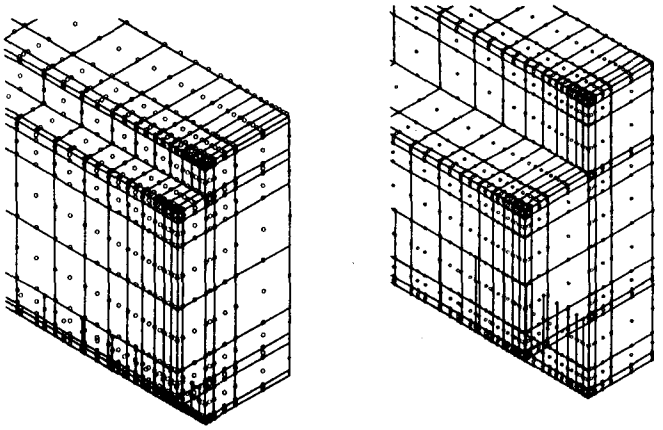

(a) (b)

FIG. 2(a - b)
Mesh generation and configuration of cross shaped ducts,
(a)- $\lambda = 0.25$ (b)- $\lambda = 0.50$

Results and Discussion

Fig. 3(a-b) displays the center-plane velocity profile and dimensionless maximum velocity through square duct (specific case of cross-shaped duct, $\lambda = 0.0$) obtained in this investigation and the experimental results of Goldstein and Kreid [7]. They made laser Doppler anemometer measurements in a square duct with water as the working fluid. The results of this study are in very close agreement with those of Goldstein and Kreid. Fig. 3b also includes the numerical results of Lawal [8] for different power law indices.

Table 1 presents the fully developed values of the key flow characteristics and Nusselt number. This table contains the results of Kozicki et al. [9] who introduced a new Reynolds number for which the relationship $f = {}^{16}/_{Re'}$ is applicable for fully developed laminar flow of a power law fluid through non-circular channels of uniform cross section. This table also includes the computational results of Gao and Hartnett [10] for the hydrodynamically and thermally fully developed condition and for various power law indices. Table 1 includes the results of Chandrupatla [11] for different boundary conditions. This table

demonstrates very good agreement between the results of this work and other available data in the literature.

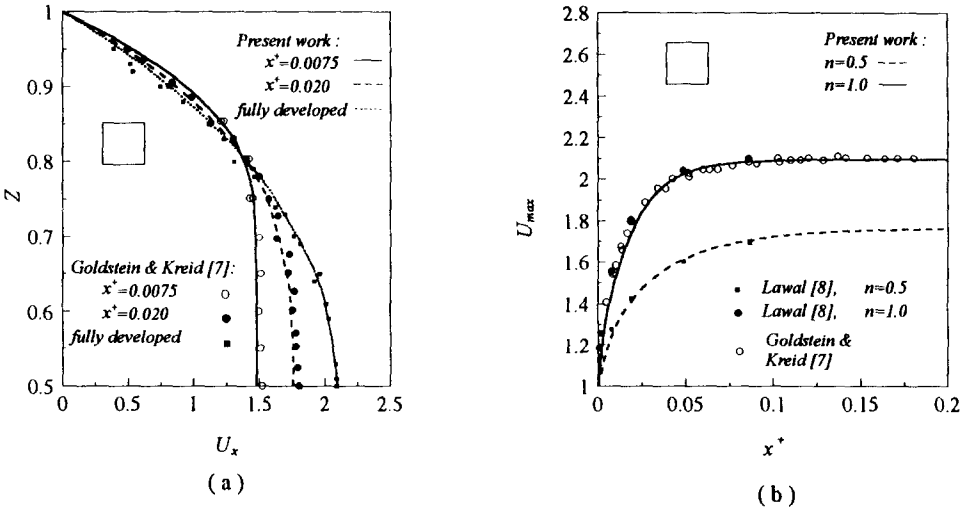

FIG. 3(a-b)
Comparison of dimensionless center-plane axial velocity profile and U_{max} : square duct

TABLE 1
Comparison of the Fully Developed Flow and Heat Transfer Characteristics for Square Duct: Present Study and Other Available Results

		f.Re	U_{max}	Nu_T	Nu_{H2}
n=0.5	*Kozicki et al. [9]*	*5.935*	---	---	---
	Chandrupatla [11]	*5.733*	*1.763*	*3.184*	*3.274*
	Gao & Hartnett [10]	*5.723*	---	---	*3.309*
	Present Study	*5.772*	*1.760*	*3.190*	*3.310*
n=1.0	*Kozicki et al. [9]*	*14.219*	---	---	---
	Chandrupatla [11]	*14.228*	*2.096*	*2.975*	*3.095*
	Gao & Hartnett [10]	*14.229*	---	---	---
	Present Study	*14.234*	*2.092*	*2.979*	*3.090*
n=1.25	*Kozicki et al. [9]*	*21.858*	---	---	---
	Present Study	*22.248*	*2.209*	*2.925*	*3.032*

For simultaneous development of flow and heat transfer Fig. 4 compares the results of this study with the results obtained by Chandrupatla [11]. $Nu_{T,x}$ has not been reported by Chandrupatla [11], hence for the T boundary condition comparison is made with $Nu_{T,m}$ reported by Chandrupatla [11]. The agreement between the two results is good.

Effect of Power-Law Index

$f_{app}Re$ for different power law indices through cross-shaped channels are presented in Fig. 5. Also the fully developed flow and heat transfer characteristics for different power law indices and various geometries are given in Table 2.

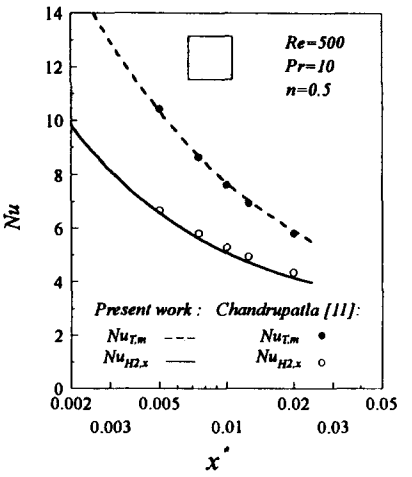

FIG. 4
Comparison of Nusselt number: square duct

Due to the flatter velocity profile for lower power law index, U_{max} decreases with decreasing n values. From Fig. 5 and Table 2 it is observed that lower n results in lower $K(x)$ and $K(\infty)$, but higher L^+. Also the power law index has a significant effect on the pressure drop. The lower apparent viscosity close to the walls for shear-thinning fluids causes smaller dimensionless pressure drop in comparison with that due to a shear thickening fluid for the same Re. Thus, from Fig. 5 and Tables 2 two important observations can be made concerning the apparent friction factor; entrance region and power law index. The hydrodynamically developing section has a higher $f_{app}Re$ than the fully developed condition. For example at $x^+ = 0.0020$, increasing power law index from 0.5 to 1.0 enhances apparent friction factor 249 % and 258 % for ducts with $\lambda = 0.25$ and $\lambda = 0.50$ respectively. These effects decrease far in downstream in such a way that the corresponding values for fully developed friction factor is 137 % and 140 %.

Fig. 6(a-d) and Table 2 show the local Nusselt number and dimensionless bulk temperature as well as fully developed Nusselt numbers for different power law indices and for T and H2 boundary conditions. Generally the Nusselt number for both T and H2 boundary conditions increases with decreasing n because of the steeper velocity gradient in the wall region for lower n values. Due to flow development, this difference decreases further downstream. For instance at $x^* = 0.00020$, Nu_T values for n=0.5 possesses about 40 % and 30 % higher value than that of Nusselt numbers belong to n=1.0 for $\lambda = 0.25$ and $\lambda = 0.50$ respectively. The corresponding values for hydrodynamically and thermally fully developed case are about 8 % and 7 %. Correspondingly Nu_{H2} for n=0.5 at $x^* = 0.00020$ are 34 % and 29 % higher than that of Newtonian fluid for $\lambda = 0.25$ and $\lambda = 0.50$. At fully developed condition these values are about 7 % and 6 %.

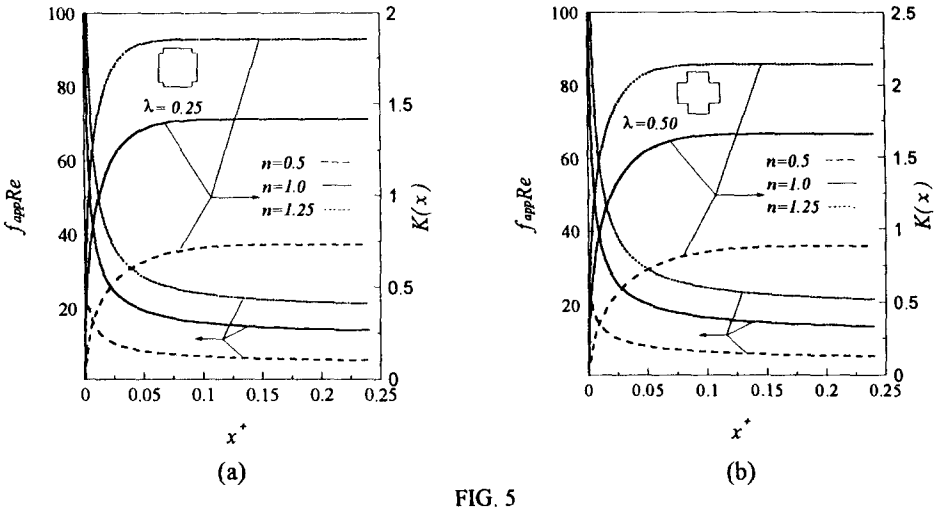

FIG. 5

Product of apparent friction factor and Reynolds number ($f_{app}\,Re$) and incremental pressure drop ($K(x)$) vs. dimensionless axial distances for different power law indices and various cross-shaped channels, $Re=500$

TABLE 2
Comparison of Flow and Heat Transfer Characteristics for Cross-Shaped Ducts with Different Geometric Parameters

		$f.Re$	U_{max}	$K(\infty)$	L^+	Nu_T	Nu_{H2}
$n=0.5$	$\lambda=0.00$	5.772	1.760	0.901	0.131	3.190	3.310
	$\lambda=0.25$	5.317	1.711	0.727	0.130	2.883	3.170
	$\lambda=0.50$	5.209	1.821	0.881	0.159	2.508	2.598
$n=1.0$	$\lambda=0.00$	14.234	2.092	1.670	0.071	2.979	3.090
	$\lambda=0.25$	12.625	2.034	1.404	0.074	2.667	2.956
	$\lambda=0.50$	12.479	2.171	1.648	0.097	2.338	2.443
$n=1.25$	$\lambda=0.00$	22.248	2.209	2.222	0.050	2.925	3.032
	$\lambda=0.25$	19.356	2.148	1.835	0.053	2.628	2.903
	$\lambda=0.50$	19.349	2.287	2.121	0.068	2.300	2.413

For the H2 boundary condition, $\theta_{b,x}$ is not affected by n. This can be explained by the fact that the heat flux is the same for different power law indices, therefore the difference in velocity profiles for different n's is not reflected in the bulk temperature. Generally for the T boundary condition and for circular cross-sectional ducts as well as parallel plates the temperature of the fluid close to the walls approaches the wall temperature; so the temperature gradient of the fluid at the wall is smaller for the T boundary condition than that for the constant heat flux case. This results in a lower Nusselt number for the former case. This difference in Nusselt numbers for a duct with sharp corners is different compared to round ducts or parallel plate channels. For ducts with sharp corners fully developed Nusselt numbers for both T and H2 boundary conditions are lower than those for circular tubes and parallel plates, but the

decrease in Nusselt numbers due to the presence of sharp corners is more pronounced for H2 than for the T boundary condition.

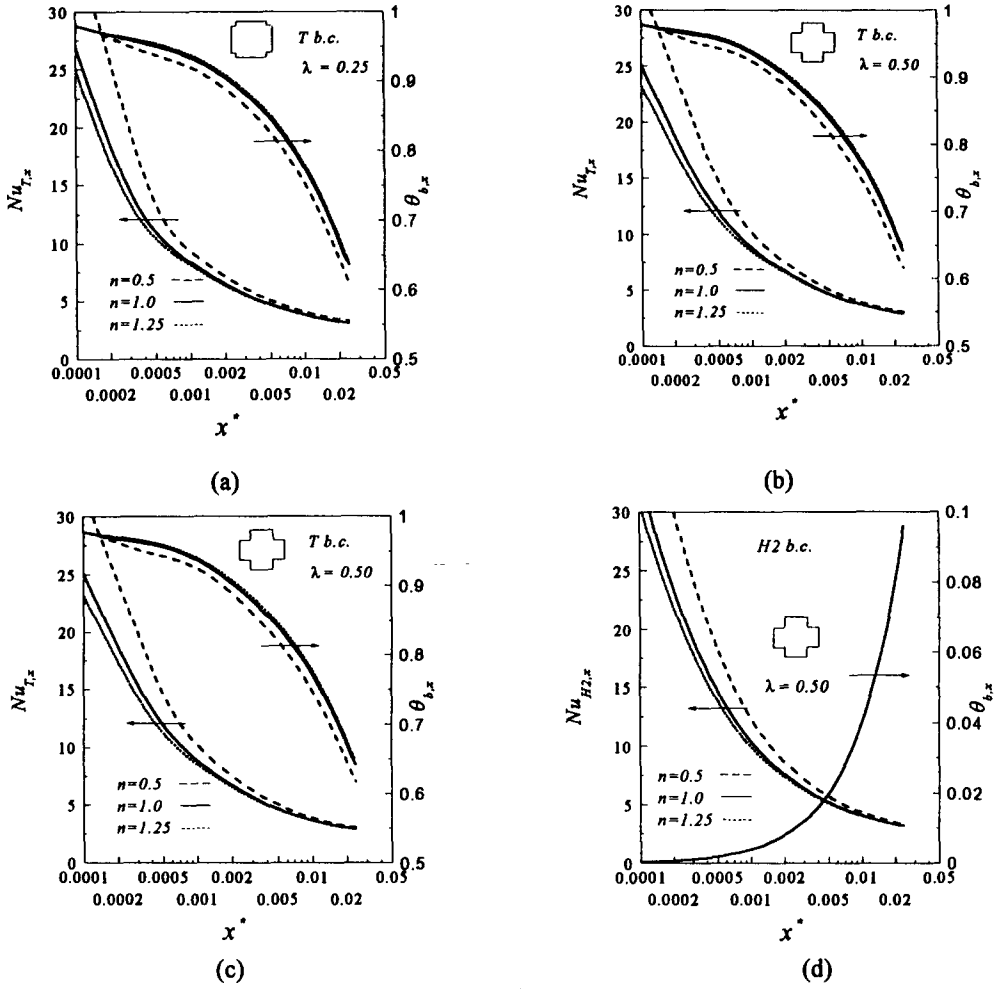

FIG. 6(a-d)
Nusselt number and dimensionless bulk temperature vs. dimensionless axial distance for different power law indices and various cross-shaped channels, *Re=500, Pr=10*

Effect of Geometric Parameter of Cross-Shaped Duct

The effect of the geometric parameter, λ, on the flow and thermal performance of cross-shaped ducts is studied numerically for *Re=500* and *Pr=10*. Fig. 7(a - d) and Fig. 8(a - d) present U_{max}, $f_{app}Re$, and Nusselt number distributions, respectively, for different values of the geometric parameter (λ). The fully developed values for selected fluid flow and heat transfer characteristics are displayed in Table 2.

From Fig. 7, U_{max} for a square duct ($\lambda = 0.0$) falls within the corresponding range for a cross-shape duct with $\lambda = 0.25$ and $\lambda = 0.50$. Also, for $n=0.5$, the square duct ($\lambda = 0.0$) yields the highest $f_{app}\,Re$ in the entrance region while the cross-shaped duct with $\lambda = 0.5$ yields the lowest value. Further downstream the lowest value corresponds to the cross-shaped duct with $\lambda = 0.25$. For Newtonian fluids the highest pressure drop is presented by square duct and the lowest value by the cross-shaped channel ($\lambda = 0.25$) over most of the axial length.

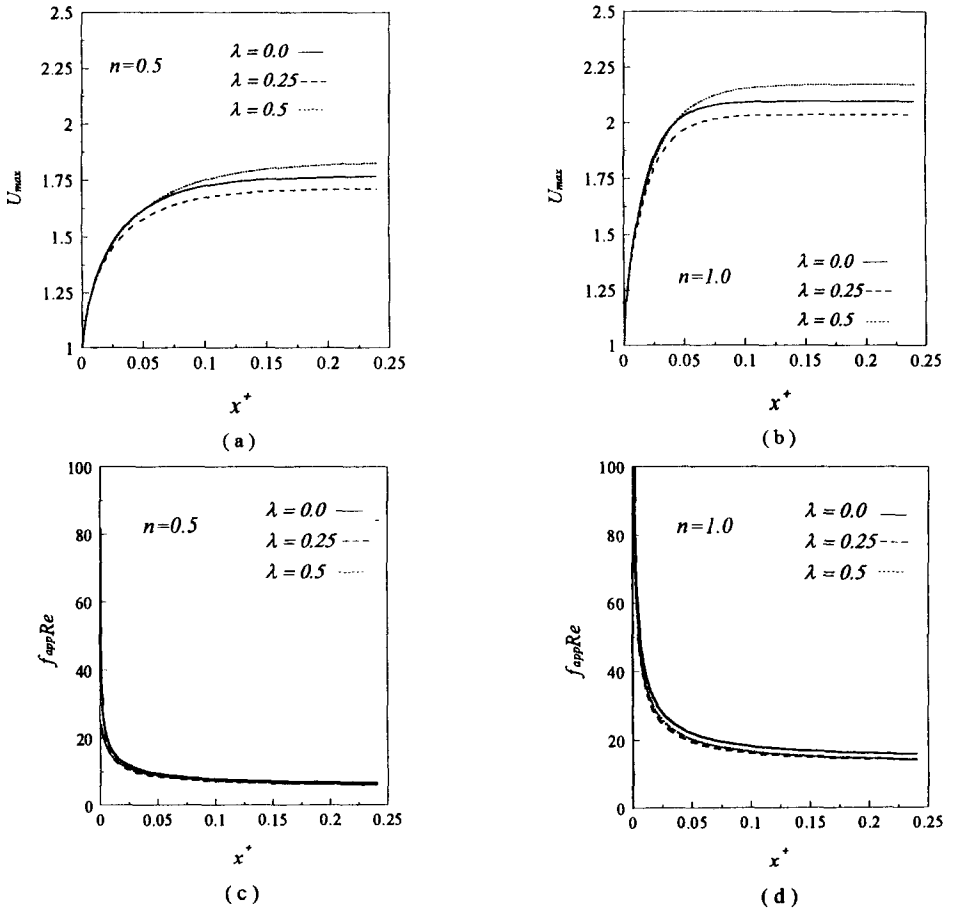

FIG. 7(a-d)
Effect of geometric parameter of cross-shaped duct on dimensionless maximum velocity and apparent friction factor, $Re=500$

For both T and H2 boundary conditions the choice of duct geometry with higher Nusselt number depends on the axial length. For example, for $n=0.5$ at $x^*=0.0002$ the highest $Nu_{T,x}$ is obtained with a cross-shaped channel with $\lambda = 0.25$ while the lowest one with a square duct. Far downstream, the square duct has the highest $Nu_{T,x}$ while the lowest $Nu_{T,x}$ is due to the cross-shaped channel with $\lambda = 0.5$. The fully

developed values of Nu_T (Table 2) emphasize the significant effect of the geometric parameter, λ, on heat transfer.

For the H2 boundary condition, close to the entrance the relative thermal performance of the duct depends on the power law index. For instance, at $x^*=0.0002$ the highest Nusselt number for $n=0.5$ is due to the square duct while the lowest value is given by the cross-shaped channel with $\lambda = 0.5$. Further downstream for both $n=0.5$ and $n=1.0$ the square duct has the highest $Nu_{H2,x}$ while the cross-shaped duct with $\lambda = 0.5$ yields the lowest value. Different behavior of the fluid flow and heat transfer characteristics can be related to number of the presence of sharp corners and velocity gradient in the corner region. In general the cross-shaped duct has the advantage of lower friction factor but it results in a lower Nusselt number.

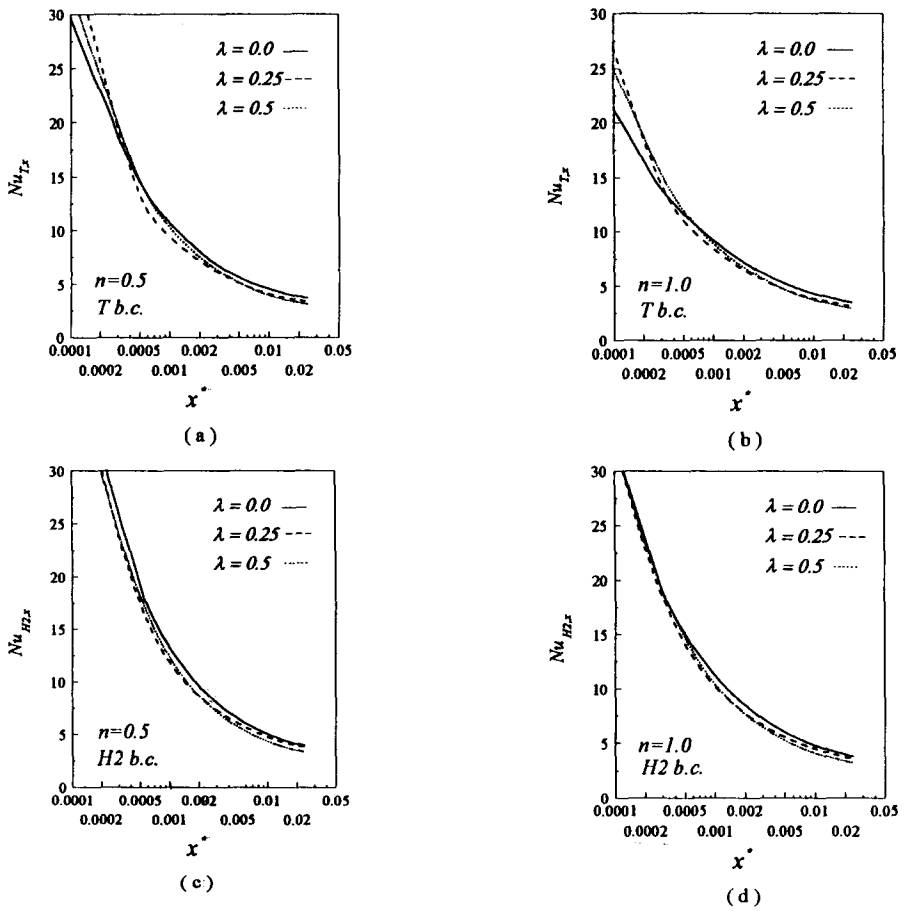

FIG. 8(a-d)
Effect of the geometric parameter of cross-shaped duct on the local Nusselt number distribution, $Re=500$, $Pr=10$

Conclusions

Numerical results for the steady laminar fluid flow and heat transfer under hydrodynamically and thermally developed as well as simultaneously developing conditions of Newtonian and power-law model non-Newtonian fluids flowing through cross-shaped channel were presented. The analysis considered the effects of the power law index under both T and H2 boundary conditions. The favorable comparison of the present result with available experimental data as well as analytical and numerical results supports the accuracy of this study.

This work has shown that the influence of the entrance region of the channels and also the effect of the power law index and geometric parameter on the flow and heat transfer characteristics can be significant. $f_{app}Re$ for pseudoplastic fluids is appreciably lower than that for dilatant fluids. For both boundary conditions the local Nusselt number for lower power law index is noticeably higher.

Acknowledgments

The financial support of Isfahan University of Technology (in Islamic Republic of Iran) is gratefully acknowledged.

Nomenclature

a	Side length of the channel
A_c	Cross-sectional area
C_p	Heat capacity
D_h	Hydraulic diameter ($= \frac{4A_c}{p'}$)
f	Friction factor ($= \frac{\tau_w}{\frac{1}{2}\rho u_e^2}$)
f_{app}	Apparent friction factor
g	Gravity acceleration
K	Thermal conductivity
k	Consistency index
$K(x)$	Dimensionless incremental pressure drop
$K(\infty)$	Dimensionless incremental pressure drop for fully developed condition
l	Hydrodynamic entrance length
L^+	Dimensionless hydrodynamic entrance length ($= \frac{l}{D_h Re}$)
n	Power law index
N	Dimensionless normal distance
Nu_{H2}	Fully developed Nusselt number for H2 boundary condition

Nu_T Fully developed Nusselt number for T boundary condition

Nu_x Local Nusselt number ($Nu_x = \dfrac{\left(\dfrac{\partial \theta}{\partial N}\right)_{w,m}}{\theta_{w,m} - \theta_{b,x}}$ for H2 and

$Nu_x = \dfrac{\left(\dfrac{\partial \theta}{\partial N}\right)_{w,m}}{\theta_{b,x}}$ for T boundary conditions)

p pressure

P Dimensionless pressure ($= \dfrac{p - \rho g z}{\rho u_e^2}$)

p' Perimeter of the channel

Pr Prandtl number ($= \dfrac{kC_p\left(\dfrac{u_e}{D_h}\right)^{n-1}}{K}$)

q Wall heat flux

Re Reynolds number ($= \dfrac{\rho u_e^{2-n} D_h^n}{k}$)

T Temperature

u Axial velocity

U Dimensionless axial velocity ($= \dfrac{u}{u_e}$)

U_{max} Dimensionless maximum velocity

v Velocity in y direction

V Dimensionless velocity in y direction ($= \dfrac{v}{u_e}$)

w Velocity in z direction

W Dimensionless velocity in z direction ($= \dfrac{w}{u_e}$)

x Axial distance

X Dimensionless axial distance ($= \dfrac{x}{D_h}$)

x^+ Dimensionless axial coordinate ($= \dfrac{x}{D_h Re}$)

x^* Dimensionless axial coordinate ($= \dfrac{x}{D_h Re.Pr}$)

y Transverse distance

Y Dimensionless transverse distance ($= \dfrac{y}{D_h}$)

z Transverse distance

Z Dimensionless transverse distance ($= \dfrac{z}{D_h}$)

Greek symbols

θ Dimensionless temperature ($= \dfrac{T - T_w}{T_e - T_w}$ for T and $= \dfrac{T - T_e}{\dfrac{qD_h}{K}}$

	for H2 boundary conditions)
λ	Geometric parameter of cross-shape channel
ρ	Density
τ	Shear stress tensor

Subscripts

b,x	Evaluated at bulk temperature and at local x position
e	Evaluated at inlet condition
$H2,x$	Evaluated at local x position for H2 boundary condition
T,x	Evaluated at local x position for T boundary condition
T,m	Mean value for T boundary condition
w	Evaluated at wall condition
x	Evaluated at local x position

References

1. R.K. Shah and A.L. London, Laminar Flow Forced Convection in Ducts. *Advances in Heat Transfer* ed. by T.F. Irvine, Jr. and J.P. Hartnett, Academic press, New York (1978).

2. R.K. Shah and M.S. Bhatti, Laminar Convection Heat Transfer in Ducts. *Handbook of Single-Phase Convective Heat Transfer* ed. by S. Kakac, R.K. Shah and W. Aung , p.3.1, John Wiley & Sons (1987).

3. Y.I. Cho and J.P. Hartnett, Non-Newtonian Fluids. *Handbook of Heat Transfer Applications* ed. by W.M. Rohsenow, J.P. Hartnett and E.N. Gonic, McGraw Hill Book Co. (1985).

4. J.P. Hartnett and M. Kostic, Heat Transfer to Newtonian and Non-Newtonian Fluids in Rectangular Ducts. *Advances in Heat Transfer* ed. by T.F. Irvine, Jr. and J.P. Hartnett, 19, p.247, Academic press, New York (1989).

5. A. Lawal and A.S. Mujumdar, Laminar Duct Flow and Heat Transfer to Purely Viscous Non-Newtonian Fluids. *Advances in Transport Processes* ed. by A.S. Mujumdar and R.A. Mashelkar, p.352, Wiley Eastern, New Dehli (1989).

6. S.Gh. Etemad, Laminar Heat Transfer to Viscous non-Newtonian Fluids in Non-Circular Ducts. *Ph.D. Thesis, McGill University, Montreal, Quebec, Canada,* (1995).

7. R.J. Goldstein and D.K. Kreid, *J. Appl. Mech.*, 34, p. 813, (1967).

8. A. Lawal, Laminar Flow and Heat Transfer to Variable Property Power-Law Fluids in Arbitrary Cross-Sectional Ducts. *Ph.D. Thesis, McGill University, Montreal, Quebec, Canada,* (1985).

9. W. Kozicki, C.H. Chou and C. Tiu, *Chem. Eng. Sci.*, 21, p.665, (1966).

10. S.X. Gao and J.P. Hartnett, *Int. Comm. Heat Mass Transfer,* 19, p.673, (1992).

11. A.R. Chandrupatla, Analytical and Experimental Studies of Flow and Heat Transfer Characteristics of a Non-Newtonian Fluid in a Square Duct. *Ph.D. Thesis, Indian Institute of Technology, Madras, India,* (1977).

Received February 7, 1997